11nd International Conference of Mechanical Engineering COMEC 2023 VI SYMPOSIUM OF COMPUTER AIDED DESIGN AND ENGINEERING, BIOMECHANICS AND MECHATRONICS

Causes of cracks appearance in fuel transport rail-tank

Causas del surgimiento de grietas en Ferro-Cisterna de transporte de combustibles

César A. Chagoyen Méndez[1], David Amauris Moreno Alonso[1], Eusebio V. Ibarra Hernández[2], Eusebio E. Pérez Castellanos[1], Juan A. Pozo Morejón[1], Sergio L. Jauregui Rigó[1], Gilberto García del Pino[3], Ángel S. Machado Rodríguez[1]

1- César A. Chagoyen Méndez. E-mail: cachagoyen@uclv.edu.cu, David Amauris Moreno Alonso. E-mail: dmalonso@uclv.cu, Eusebio E. Pérez Castellanos. E-mail: eusebiopc@uclv.edu.cu, Juan A. Pozo Morejón. E-mail: jpozo@uclv.edu.cu, Sergio L. Jauregui Rigó. E-mail: jaureguisl@uclv.edu.cu, Ángel S. Machado Rodríguez. E-mail: angelmr@uclv.edu.cu, Facultad de Ingeniería Mecánica e Industrial, Universidad Central "Marta Abreu" de Las Villas. Cuba.

2. Eusebio V. Ibarra Hernández. Facultad de Ing. Química y Farmacia, Universidad Central "Marta Abreu" de Las Villas. Cuba, E-mail: eusebioih@uclv.edu.cu

3. Gilberto García del Pino. Coordenação de Engenharia Mecânica. Universidade do Estado do Amazonas, Manaus, Brasil, E-mail: gpino@uea.edu.br

Abstract:

• **Problem to deal with:** This paper presents an analysis of the failures that occur in several rail-tankers that are used to transport fuel.

• **Aims:** Determine the causes of the failures in the cylindrical part of the cistern and in the ends of the holes of the side beams.

• **Methodology:** The stress behavior of the finite element model made under the operating loads is simulated. The tensional and deformational state of the zones where the faults occur is deepened in order to know the influence of the same in the appearance of the cracks.

• **Results and discussion:** The results obtained fully coincide with the real failure situation that occurs in the analyzed ferro-tanker, that is, the failure in the container is evident in the area of the welded joints in the channel-type reinforcement rings, as well as in the screw holes at the ends of the side beams.

• **Conclusions:** As possible causes of the appearance of failures are the fixing by screws in the side beams and the use of split channel-type reinforcements.

Resumen:

- ***Problemática:*** *En este trabajo se presenta un análisis de las fallas que ocurren en varias ferro-cisternas que se emplean para el transporte de combustible.*
- ***Objetivo:*** *Determinar las causas de las fallas en la parte cilíndrica de la cisterna y en los extremos de los agujeros de las vigas laterales.*
- ***Metodología:*** *Se simula el comportamiento tensional del modelo de elementos finitos confeccionado bajo las cargas de operación. Se profundiza en el estado tensional y deformacional de las zonas donde ocurren las fallas para conocer la influencia del mismo en el surgimiento de las grietas.*
- ***Resultados y discusión:*** *Los resultados obtenidos coinciden plenamente con la situación real de falla que ocurre en la ferro-cisterna analizada, es decir, se evidencia la falla en el recipiente en la zona de las uniones soldadas en los anillos de refuerzo tipo canal, así como en los orificios de los tornillos en los extremos de las vigas laterales.*
- ***Conclusiones:*** *Como posibles causas de aparición de las fallas se encuentra la fijación por tornillos en las vigas laterales y el empleo de refuerzos tipo canal partidos.*

Keywords: Rail-tankers; Failures; Cracks; ASME Code; Numerical Simulation
Palabras Clave: *Ferro-cisternas; Fallas, Grietas; Código ASME; Simulación Numérica*

1. Introduction

Fuel transportation has always been one of the most influential problems in the world economy. Therefore, various forms of transportation have been developed such as wagons, trucks, tankers and pipelines. The method used to move these fuels depends on the quantity to be moved and the distance to the destination. The biggest problems with this move are contamination and the possibility of spillage.

Rail-tankers are rail vehicles intended for the bulk transportation of liquid, solid or gaseous products and are another way of moving crude oil by land.

The fuel is loaded onto tank cars and moved by a diesel train across the rails to the refinery or planned destination. Rail-tankers and trains are a common way to transport large amounts of fuel by using several tank cars over long distances. They provide services for the transfer of fuels from the unloading ports to the different consumer entities. The rail-tank model that is analyzed in this work was imported from the year 2008, with the purchase of 250 pieces of equipment. They were started up and in some cases their use was changed for the transfer of alcohols, cement and oils.

The rail-tankers are classified as pressurized, non-pressurized and for the transport of cryogenic liquids. The non-pressurized ones, as is the case at hand (also called "general service" or "low pressure" tank cars), are used to transport a wide variety of liquid and solid products [3].

Failure have been detected in these vehicles, specifically the appearance of eight cracks in the cylindrical part of the tank, inside the four reinforcements on both sides of the vessel and at the same height. Failure also occurs at the bolt holes at the ends of the lateral beams.

This work deals with vessel that move long distances on a chassis along railway tracks, almost 12 meters long and almost 3 meters in diameter, with more than 72 m^3 of fuel, spilling out for initially unknown causes.

That is why it is decided to study and detect possible deficiencies in the design, carry out the analytical calculation using the ASME code and simulate the stress behavior of the finite element model made under operating loads to determine the possible causes of the appearance of cracks.

Common pressure vessel codes used for design are: ASME Boiler and Pressure Recipient code section VIII, European Committee for Standardization and British Standards Institution. The ASME code is used for the design and construction of equipment subjected to vacuum, low, medium and high pressure. This code is widely accepted worldwide and is undoubtedly the most widely used in our region. [3].

The main stresses that arise in horizontal vessels supported on saddles are longitudinal, shear, and circumferential stresses [6]. Zick [16] indicated the approximate stresses that

exist in cylindrical vessels supported on two supports. He showed that by knowing the stresses it is possible to know which vessels can be designed for the internal pressure alone. Moss [10] explained the detailed design process for horizontal pressure vessels and saddle support design for large vessels.

Ong and Lu [13] suggested a parametric study for the determination of the optimum loose-fitting saddle support radius for cylindrical pressure vessels. Diamantoudis *et al*. [4] did a comparative design study using different finite element techniques. El-Abbasi et al. [5] carried out a three-dimensional finite element analysis of a pressure vessel resting on flexible supports. Works such as that of Nayak et al. [12], that of Leyva-Díaz [7] and that of Nash et al. [11] have in common the use of the finite element method. They applied as external loads to the model the own weight, the weight of the filled liquid and the internal pressure, in the same way that is done in this work.

In this work, graphical and numerical results are obtained for seven load cases. The results obtained fully coincide with the reality of the failure that occurs in the rail-tank.

2. Methodology

2.1 Finite Element Model

Geometric model of the component parts of the rail-tank

From in situ measurements of the rail-tank studied in the workplace (figure 2.1) and taking into account some measurements recorded in the equipment History Book [15], the geometric model was created.

Figure 2.1 Image of rail-tank studied. Source: (author)

For the creation of the geometric model, the analyzed rail-tank was divided into its component parts as shown in figure 2.2.

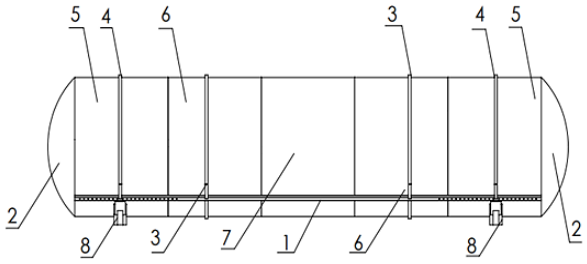

Figure 2.2 Geometric representation of the model and its components. Source: (author)

The model is divided into the following components, as indicated by the numbering:

- ✓ Two rolls (5), one at each end that also contain the head (2).
- ✓ Three central rolls (6 and 7).
- ✓ Two side T-beams (1) with 24 screw holes at both ends.
- ✓ Four channel-type reinforcing rings. The inner rings (3) cover the entire perimeter of the surface. While those at the ends (4) do not cover it, since they reach the intersection with the lateral T beams since the saddle-type supports are found in that plane.
- ✓ Two saddle-type support structures, made up of wear plates (reinforcement), one fixed to the vessel (8) and the other to the saddle, as well as other plates arranged vertically.

These elements are joined by welding, and can be simulated in *SolidWorks* [14] as a global contact by rigid union.

Boundary Conditions Definition

In this model there are several restriction zones that condition the operation of the equipment. As a first condition, it presents a fixed geometry on the lower faces of the supports that represents the union of these to the chassis of the equipment. It also features fixed fastening at 96 bolt holes spaced 100mm from the ends of the two side T-beams. These beams are welded to the vessel and bolted to a sheet frame that is fixed to the chassis. Figure 2.3 a) and b) show the application of both conditions.

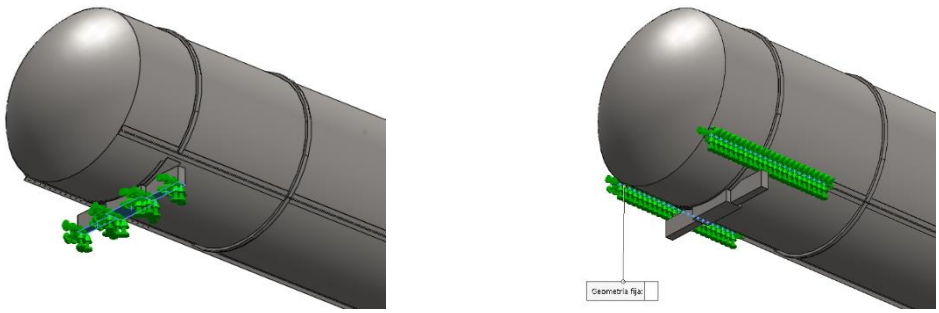

a) b)

Figure 2.3 a) Fixed geometry condition at the supports.
b) Fixed geometry condition at ends of lateral beams. Source: (author)

Load Cases Definition

The main loads that are taken into account in this equipment are: the pressure of the liquid, its weight and the structure's own weight. In this research several simulations of the influence of these loads are presented, analyzing their static and dynamic behavior with water and fuel, under test and operating pressure conditions. In addition, the load considerations raised in the ASME code for these vessels are taken into account. Finally, 7 load cases were established:

A. Static Load: the stationary vessel

*Load case **1***: the following loads were considered:
- Test pressure with uniform distribution (0.2 MPa).
- Own weight of the vessel.
- Weight of the liquid (water).

*Load case **2***: the following loads were considered:
- Hydrostatic pressure with non-uniform distribution (0.0274 MPa).
- Own weight of the vessel.
- Weight of liquid (fuel)

B. Dynamic Loads: the vessel in motion.

*Load case **3***: The following loads must be considered:
- Hydrostatic pressure with non-uniform distribution (0.0274 MPa).
- 1.35 of the weight of the vessel in the vertical direction.
- 0.35 of the weight of the vessel in the longitudinal direction in one of the two directions.
- 0.2 of the weight of the vessel in the transverse direction placed at the vertical center of gravity.

*Load case **4***: The following loads must be considered:
- Hydrostatic pressure with non-uniform distribution (0.0274 MPa).
- 1.42 of the weight of the vessel in the vertical direction.

*Load case **5***: The following loads must be considered:
- Hydrostatic pressure with non-uniform distribution (0.0274 MPa).
- Own weight of the vessel.
- 0.7 of the Weight of the vessel in the longitudinal direction in one of the two directions.

*Load case **6***: The following loads must be considered:
- Hydrostatic pressure with non-uniform distribution (0.0274 MPa).
- Own weight of the vessel.
- 0.4 of the weight of the vessel in the transverse direction placed at the vertical center of gravity.

*Load case **7***: The following loads must be considered:
- Hydrostatic pressure with non-uniform distribution (0.0274 MPa).
- Own weight of the vessel.
- 2 of the weight of the vessel in the longitudinal direction distributed in one of the head, in one of the two directions.

Material Definition and its Properties

The rail-tank material was obtained from his History Book [15]. This document reflects the structural steel St 37-2 (DIN 1.0037) [8], which is equivalent to ASTM A36 Grade

D and ASTM A284 Grade D steels. Table 2.1 shows the chemical composition and table 2.2 the main physical and mechanical properties of this steel.

Table 2.1 Chemical properties of St 37-2 steel. Source: [8]

Al	S	C	P
0.02	0.04	0.17	0.04

Table 2.2 Main physical and mechanical properties of St 37-2 steel. Source: [8]

Properties	Value	Units
Modulus of Elasticity	210000	N/mm^2
Poisson's Ratio	0.28	N/D
Shear Module	79000	N/mm^2
Density	7800	kg/m^3
Tensile strength	360	N/mm^2
Yield strength	235	N/mm^2

Finite Element Mesh

A high-quality mesh of solid elements was defined, using a compatible curvature-based mesh for contacting or partially contacting edges of the sheet metal and surface bodies. The size of the elements of said mesh ranges between 50 and 10 millimeters (maximum and minimum) for a total of 463'440 elements and 149'208 nodes. This finite element mesh was validated, that is, 3 meshes were made: one fine, one medium and one coarse, and the simulation was executed for each of them. A locus was chosen in which the von Mises stress value was obtained for each run. The difference between said tension values between two consecutive analyzes did not exceed 5%, indicating that the precision is adequate. Therefore, in this particular case of analysis, the average mesh was used, which is also the one proposed by SolidWorks [14], which was the software used.

2.2 Failure description

The problem or failure was described initially as follows: "The appearance of 8 cracks in the cylindrical part of the rail-tank, inside the four channel-type reinforcements on both sides of the vessel and at the same height". Subsequently it is known that exactly in the failure zone there is a tie, by welding, of the reinforcing channel, that is to say that the channel is not one-piece but split. Said union is made in the area where the deformations are considerable, later verified with the simulations carried out and the diagrams that appear in the ASME code that occur mainly in the lateral direction. Until

then, the causes of this failure are unknown. If it was absolutely necessary to split the channel, the union should have been done at the top of the vessel.

Causes that lead to failure: as the tie of the reinforcement channel is in an area where considerable deformations occur, these together with the dynamic loads that occur, cause the failure of the weld of said channel.

Welding converts both parts (channel and vessel) into one piece. For this reason, the crack begins in the external weld of the "soul" of the channel, advances towards the "skid" until it reaches the vessel, on one side, or on both sides, a crack that grows indefinitely due to the deformations caused by the loads mentioned above. This mechanism is described with images in figure 2.4.

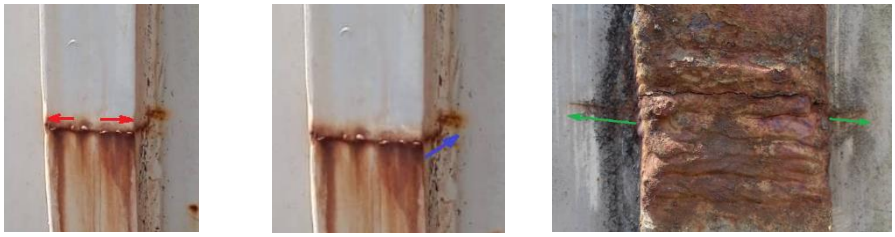

Start of the crack (soul of the channel) | Crack advance (skid of the channel) | Crack advance (vessel)

Figure 2.4 Representation with images of the failure mechanism. Source: (author)

Details of the model in the failure zone

These rail-tankers have around 15 years of exploitation. A year ago the cracks and fissures began to visualize. It is considered that their appearance is due to a fatigue process accelerated by the presence of these welded joints, which increase the deformation of the material in those locations under operating loads.

For this reason, these joints, over time, suffer fractures and their components separate, causing an increase in stress on the surface of the vessel below the ring, and consequently failure occurs.

The simulation is performed when the weld in the channel has failed and the crack has come to separate the two joint components at all 8 locations. The simulation is done in this way because it is more important to determine the stresses that arise in the vessel when the crack has separated the reinforcement channels, than the stresses in the itself reinforcement.

From the visual inspection in the failure zones, the measurements for its location in space were determined, and in this way represent it in the geometric model, taking into

account the height and the distance from the symmetry axis of the vessel as shows figure 2.5 a). To apply this condition to the model, a separation of one millimeter is made in the areas where the rings are tied, as shown in figure 2.5 b).

a) b)

Figure 2.5 a) Welded joints representation of the reinforcement channel.
b) Location of the welded joint. Source: (author)

2.4 Design deficiencies of the rail-tank detected and, at the same time, differences between the calculation model of the ASME code and the finite element model of the rail-tank studied.

In all this research, from the study of the failure, it has been possible to detect the following deficiencies in the design and construction of these rail-tankers:

1. This design takes a single thickness of 6 mm for the entire rail-tank and reinforces the body of the vessel by means of channel-type geometry rings. This thickness is relatively small if we compare it with other rail-tank of similar dimensions and capacity. There are some that vary in thickness, being greater at the bottom (greater hydrostatic pressure) and less at the top.

2. This rail-tank is fixed to the chassis at the lateral ends (on both sides) by means of 24 screws in each of them for a total of 96, which limits deformation in the longitudinal direction. It has metal supports, apparently with the idea that the vessel slides on them, but since it is fixed at the four ends we think that in practice it slides very little on said supports.

3. The original design and construction does not have any support in the center of the vessel, place where considerable displacements occur, which would be reduced if it had some type of support in the center.

4. The lower supports at the ends (figure 2.6) do not have a design and construction according to this vessel.

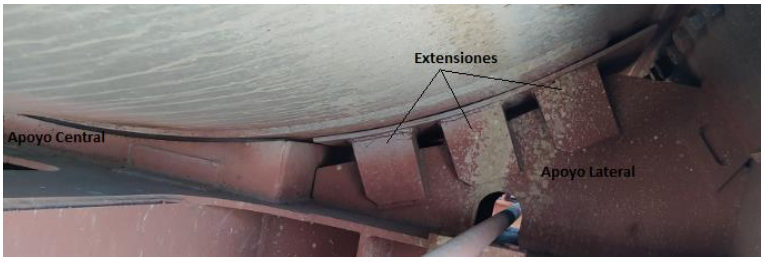

Figure 2.6 Lower supports at the ends of the rail-tank. Source: (author)

As can be seen in the previous image, the saddle is divided into three parts (central support and lateral supports). The lateral supports have "extensions" to get the supports to the vessel.

The classic saddles used as supports in most vessel are integral with the appropriate dimensions so that the vessel rests completely on the saddle, generally with reinforcements. It is impressive that the supports that this vessel has were not designed for it.

5. The angle of support of the vessel on the saddle (θ) recommended by the ASME code must be between 120° and 180°. However, in this rail-tank it is 90°.

6. About the reinforcements: their spacing, welding and use.

In Section XII of the ASME code, 2019 Edition [2], p. 205, in the Special Provisions, states verbatim:

(1) Category 406, 407, and 412 tanks of shell thicknesses less than 9.5 mm (0.375 in.) shall have circumferential reinforcement or stiffening at a maximum spacing of 150 cm (60 in.) unless designed per TD-210 for full vacuum … Such reinforcement or stiffening shall not cover any circumferential shell joint … and shall be continuous around the perimeter and welded to the shell with spaced welds for at least half the perimeter.

… Hat-shaped or open-channel ring stiffeners that prevent visual inspection of the tank shell are prohibited on Category 406, …

However, in the rail-tank being analyzed, reinforcements or open channel type stiffeners are used; these stiffeners are not continuous but divided; the spacing is a little more than 2 m, not 1.5 m, and the weld is around the entire perimeter of the vessel, not spaced. Failure to comply with these Provisions constitutes **deficiencies in the design**.

3. Results and Discussion

3.1 Numerical results of the simulation under Static Load: the stationary vessel. Load Cases 1 and 2.

Of all the possible numerical results offered by the software used for the numerical simulation, the following were chosen to make the comparison between the different load cases (L.C.): Equivalent von Mises stress, Normal stress in the X, Y and Z axes, Shear Stress in the direction of the Z axis (XZ plane), Shear Stress in the direction of the Z axis (YZ plane) (MPa), Shear Stress in the direction of the Y axis (YZ plane) (MPa), Displacements and Deformations. The results of these parameters for load cases 1 and 2 under static loads can be seen in Table 3.1.

Table 3.1 Numerical results of load cases 1 and 2. Source: Author.

Results	L.C. - 1	L.C. - 2
Equivalent von Mises stress (MPa)	886.3	1385.8
Displacements (mm)	1.3	4.7
Deformations	0.002	0.004
Normal stress in the X axis (MPa)	632.9	792.5
Normal stress in the Y axis (MPa)	531.9	602.3
Normal stress in the Z axis (MPa)	871.5	1007.4
Shear Stress in the direction of the Y axis (YZ plane) (MPa)	187.3	562.3

It is observed that in the load case 2 it is the one that reaches the highest values of stresses and displacements, the deformations are the same in both. This case has as loads the test pressure with non-uniform distribution, the own weight of the vessel and the weight of the liquid (fuel). When the graphical results are displayed, the results will be explained.

3.2 Numerical results of the simulation under Dynamic Loads: the vessel in motion. Load Cases 3, 4, 5, 6 and 7.

The results of stresses, displacements and strains for load cases 3, 4, 5, 6 and 7 under dynamic loads can be seen in Table 3.2.

Table 3.2 Numerical results of load cases 3, 4, 5, 6 y 7. Source: Author.

Results	L.C. - 3	L.C. - 4	L.C. - 5	L.C. - 6	L.C. - 7
Equivalent von Mises stress (MPa)	1414,6	1422,6	1400,9	1324,1	1401,8
Displacements (mm)	4,8	4,8	4,7	4,7	4,7
Deformations	0,004	0,004	0,004	0,004	0,004
Normal stress in the Z axis (MPa)	1030,3	1035,7	994.6	993,8	987,6
Shear Stress in the direction of the Y axis (YZ plane) (MPa)	581,4	584,7	575,8	542,9	587,9

If the results of table 3.2 are plotted as can be seen in figure 3.1, it can be seen that the behavior of the measured parameters is very similar for all load cases. No one prevails over another. However, load case 4 has some parameters such as the von Mises stress and the normal stress in the X and Z axes above the rest. In this load case, the non-uniform hydrostatic pressure of fuel and an increase of 42 percent of the gravity load in the vertical direction were considered as load.

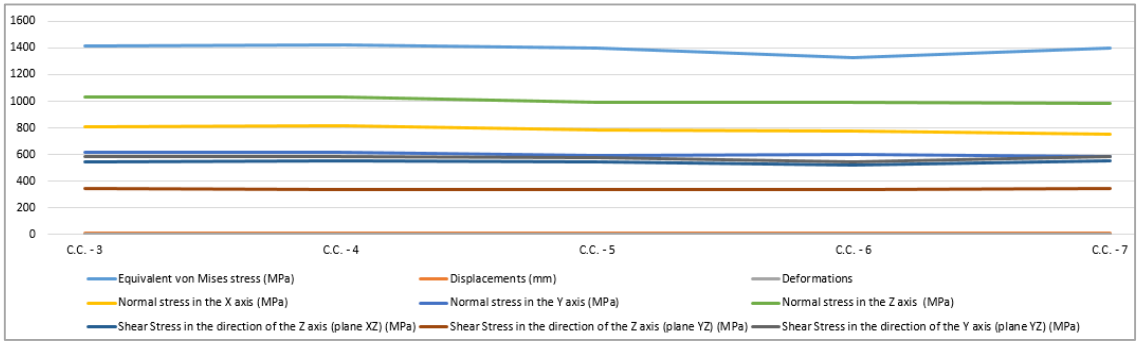

Figure 3.1 Load case comparison 3, 4, 5, 6 y 7

3.3 Graphical results of the simulation for Load Case 4.

As Load Case 4 is the one with the highest stress and displacement values, it will be the one for which the main graphic results will be shown.

von Mises stresses

Figure 3.2 shows the von Mises stresses. It can be seen that the entire surface of the rail-tank is below the elastic limit of the material of 235 MPa (dark blue zone), except for the extreme hole of one of the beams where the maximum value of these stresses of 1422.6 MPa appears, which exceeds 6 times the elastic limit.

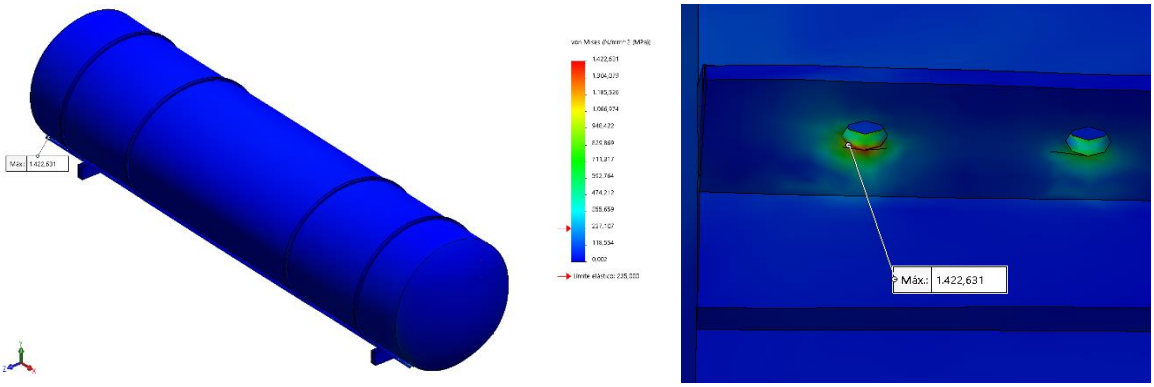

Figure 3.2 von Mises stresses distribution. Source: (author).

The maximum values of 1422.6 MPa are found in the extreme holes corresponding to fixing screws, in the lateral beams. Figure 3.2 shows details of that place, where it can

be seen that the maximum values (reddish area) exceed the elastic limit of the material, causing resistance failure in that area.

Displacements

Regarding the resulting displacements, the maximum values are 4.84 mm in the upper area in the center of the cistern. This behavior is due to the presence of fixing by screws in the lateral beams, which prevent displacements from occurring towards the ends of the rail-tank in the longitudinal direction. This means that the displacements occur mostly perpendicular to said axis, as shown in figure 3.3.

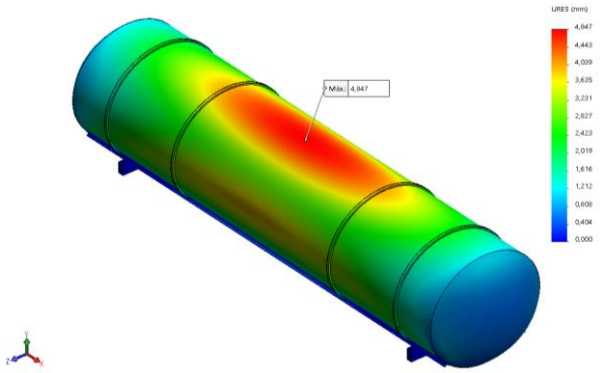

Figure 3.3 Resulting displacements. Source: (author).

Deformations

The deformations shown in figure 3.4 reflect maximum values of 0.004 in the last screw hole in one of the lateral beams. Said behavior is the same in all other end holes. It is also observed that in the rest of the equipment the values are around 0.001 (dark blue areas).

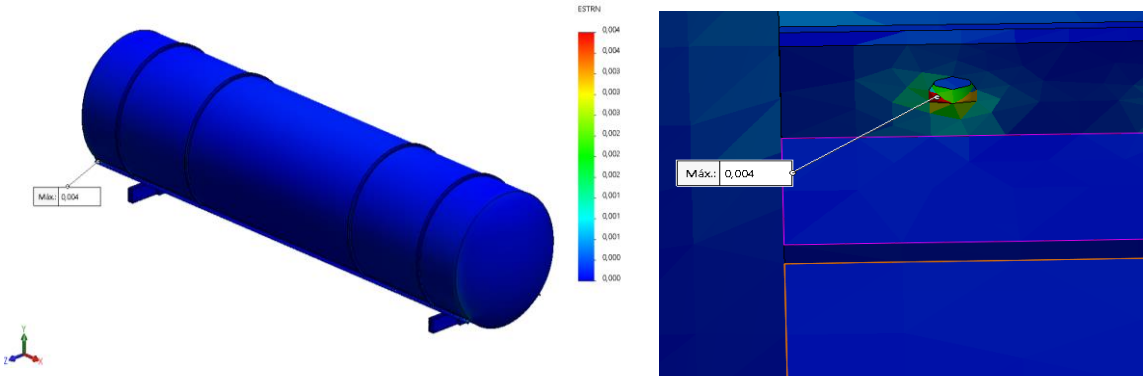

Figura 3.4 Deformations. Source: (author).

Figure 3.4 shows an enlarged detail of the area of greatest deformation, which reflects the presence of the reddened area on the lower surface of the screw hole.

Normal stresses in the Z axis

The normal stresses in the Z axis are also located perpendicular to the longitudinal axis of the rail-tank, in the horizontal direction. The highest value of 1035.7 MPa (figure 3.5) is also found in the end hole of the lateral beam and exceeds the material limit.

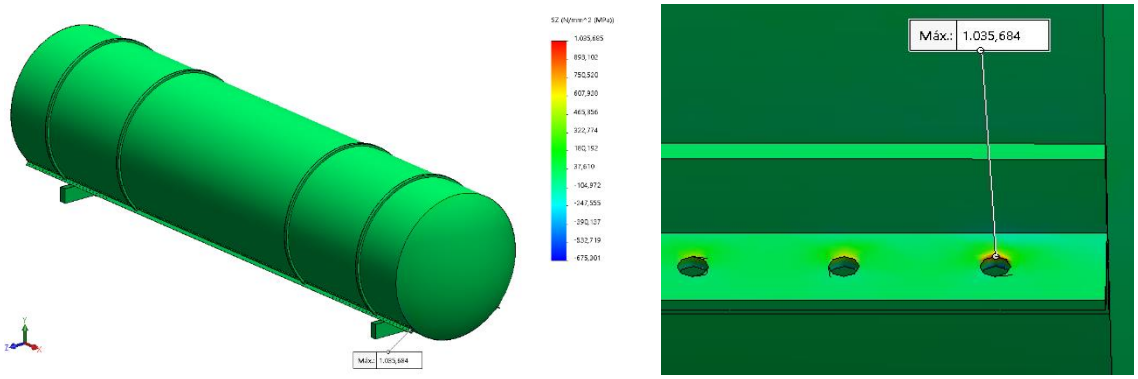

Figure 3.5 Normal stresses in Z axis. Source: (author).

Shear stresses

Figure 3.6 shows the largest shear stresses arising in the Y direction in the YZ plane of the three components (shears in XY, XZ and YZ) analyzed. The maximum value of 584.7 MPa is observed in the extreme hole of the lateral beam, which exceeds the limit of the material for this type of stress.

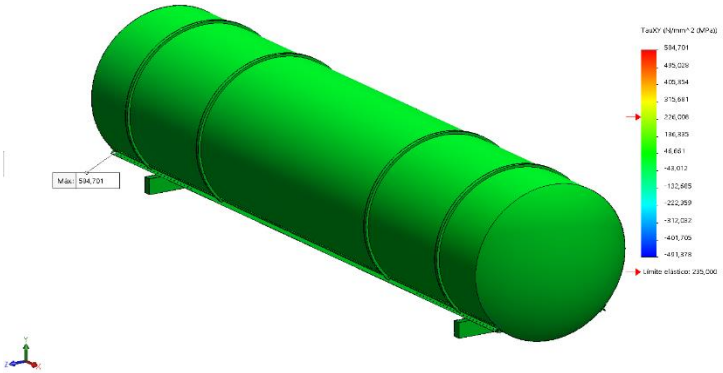

Figure 3.6 Shear stresses in the Y direction in YZ plane. Source: (author).

As shown in the results of the previous simulations, in most cases, the maximum stress values arise at the bolt holes at the ends of the side beams which exceed the allowable stresses of the material, thus occurring resistance failure. This fully corresponds to reality, since the rail-tanker being investigated has shown notable deterioration and fractures in said areas. The image in figure 3.7 shows the deterioration and the repair that has been undertaken.

Figure 3.7 Failure zone in the extreme screw hole after repaired. Source: (Author).

3.4 Numerical and graphic results in the failure zone

To analyze the failure zone, simulated from a one-millimeter gap in the tie of the rings as explained above, values are taken at selected locations. Figure 3.8 shows the analysis area and the stress value at a point in this region in the normal direction of the Y axis in an enlarged form. A maximum value of 301 MPa is observed, which is greater than the permissible value of the material (235 MPa), so the failure occurs.

Figure 3.8 Normal stresses on the Y axis in the failure zone. Source: (author).

The von Mises stresses are also shown in Figure 3.9, with maximum values in the failure zones of 253 and 251 MPa, which also exceed the allowable stress.

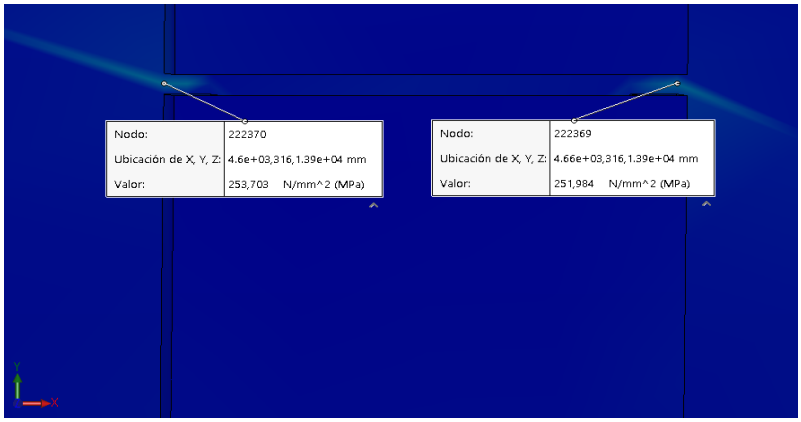

Figure 3.9 Equivalent von Mises stresses in the failure zone. Source: (author).

The simulation reflects how when the separation of the components of the welded joint (crack) occurs, tensions greater than the permissible arise on the surface under the ring (in the shell), which fully coincides with the reality that occurs in the rail-tank studied as shown in figure 2.4 "Crack advance". The image shows the defective repair of the channel type ring (which cracked again) and the growth of the crack in the vessel.

4. Conclusions

The rail-tank analyzed in this work is non-pressurized, made of St-37-2 carbon steel and is used to transport fuel. The loads considered are the own weight of the vessel, the weight due to the fuel and the pressure that this exerts on the walls of the shell. These loads cause circumferential, longitudinal and shear stresses that were simulated in seven load cases: two static and five dynamics, simulating combinations of uniform and non-uniform pressure and variations in the inertial coefficients of gravity (dynamics) according to the ASME code.

The stresses obtained by the ASME code and those obtained by numerical simulation reach values lower than the admissible stress of the material, so there is no resistance failure at the control points. This behavior can occur due to the fixation by screws of the rail-tank in the lateral beams.

In the most critical load case, the von Mises stress reaches 1,422.6 MPa at the bolt hole at the end of the lateral beams. This value is much higher than the admissible value (235 MPa) so the material failure in that zone, as it happens in reality. In the rest of the rail-tank the behavior is uniform with stress values well below the limit of the material.

The stresses obtained in the failure zone of the reinforcements or stiffeners exceed the admissible stress of the material, which fully corresponds to reality.

The results presented in this work coincide with the real situation of cracking that occurs in the analyzed rail-tank. It can be said that the following are possible causes of the appearance of cracks:

- The fixing by screws in the lateral beams, constitute embedment's that are above the level of the supports, cause the vessel to be fixed at the four lateral ends and practically does not rest on the lower supports, limiting the deformation in the longitudinal direction. This transforms the stress behavior of the vessel, causing the highest stress

values to arise in the holes of the extreme bolts, which are close to the head, and cracking occurs in that area.

- The use of split channel-type reinforcements or stiffeners, that is, with a tie by welding the channel in the area where the deformations are considerable, in addition to failing to comply with the ASME provisions and constituting deficiencies in the design, cause the appearance of cracks in the vessel.

5. Bibliographic References

[1] ASME Boiler and Pressure Vessel Code (BPVC), Section VIII - ISBN 978-0-7918-7288-8. New York, USA. 2019.

[2] ASME Boiler and Pressure Vessel Code (BPVC), Section XII - Rules for Construction and continued service of Transport Tanks. ISBN 978-0-7918-7295-6. New York, USA. 2019.

[3] ASME Boiler and Pressure Vessel Code, Section VIII, Pressure Vessels Division, 2. ED 2010.

[4] Diamantoudis A. Th., Kermanidis, Th. Design by analysis versus design by formula of high strength steel pressure vessel a comparative study. International Journal of Pressure Vessels & Piping, vol.82, pp. 43-50, 2005.

[5] El-Abbasi, N., Maguid S. A., Czekanski, A. Three dimensional finite element Analysis of saddle supported pressure vessel," International journal of mechanical sciences, vol. 43, pp. 1229-1242, 2001.

[6] Kumar, V., Kumar, N., Angra, S. Sharma, P. Design of Saddle Support for Horizontal Pressure Vessel. International Journal of Mechanical, Aerospace, Industrial and Mechatronics Engineering Vol:8 No:12, 2014.

[7] Leyva-Díaz, A., Trejo-Escandón, J. O., Flores-Herrera, L. A., Tamayo-Meza, P. A., Sandoval-Pineda, J. M. Modal Analysis of Railroad Tank Car Using FEM, International Journal of Engineering Trends and Technology (IJETT) V16(2) (Oct 2014) 49–53. ISSN: 2231-5381.

[8] MatMach 2022 GmbH (Materials Search Platform). Leopoldstraße 250 A, 80807 Munich. URL:https://matmatch.com/materials/minfc6403-din-5512-2-grade-st-37-2-g-cold-rolled Accedido: 5-11-2022.

[9] Mijalev, F. M. et al. Cálculo y diseño de máquinas y aparatos de la industria química. Vneshtorgizdat, Moscú. URSS. 1987.

[10] Moss, Dennis. R. Pressure Vessel Design Manual. Fourth edition, 2013, pp. 254-267.

[11] Nash, D. H., Banks, W. M., Bernaudon, F. Finite Element Modeling of Sling-Supported Pressure Vessels. Thin-Walled Structures, Vol. 30, nos. 1–4, pp. 95–110, 1998.

[12] Nayak, A., Singru, P. (2021). Study of Effect of Angle of Contact and Angle of Extension of Wear Plate on Maximum Stress Induced in Horizontal Pressure Vessel. In: Rao, Y.V.D., Amarnath, C., Regalla, S.P., Javed, A., Singh, K.K. (eds) Advances in Industrial Machines and Mechanisms. Lecture Notes in Mechanical Engineering. Springer, Singapore. https://doi.org/10.1007/978-981-16-1769-0_46

[13] Ong L. S., Lu, G. Optimal support radius of loose-fitting saddle. International Journal of Pressure Vessels & Piping, vol.54, pp. 465-479, 1993.

[14] SolidWorks 2020 Release. Dassault Systèmes - SolidWorks Corporation. 18-09-2019.

[15] Wagon Pars Co. History Book of Cuba fuel wagon. Arak, Irán. 2007.

[16] Zick, L. P. Stresses in large horizontal cylindrical Pressure vessel on two saddle supports. The welding Research Supplement, pp.959-970, 1971.